WATER RESOURCES RESEARCH, VOL. 44, W01432, doi:10.1029/2007WR006094, 2008

Click Here for Full Article

Onset of water stress, hysteresis in plant conductance, and hydraulic lift: Scaling soil water dynamics from millimeters to meters

Mario Siqueira,[1,2] Gabriel Katul,[1,3] and Amilcare Porporato[1,3]

Received 6 April 2007; revised 31 July 2007; accepted 2 October 2007; published 25 January 2008.

[1] Estimation of water uptake by plants and subsequent water stress are complicated by the need to resolve the soil-plant hydrodynamics at scales ranging from millimeters to meters. Using a simplified homogenization technique, the three-dimensional (3-D) soil water movement dynamics can be reduced to solving two 1-D coupled Richards' equations, one for the radial water movement toward rootlets (mesoscale, important for diurnal cycle) and a second for vertical water motion (macroscale, relevant to interstorm timescales). This approach allows explicit simulation of known features of root uptake such as diurnal hysteresis in canopy conductance, hydraulic lift, and compensatory root water uptake during extended drying cycles. A simple scaling analysis suggests that the effectiveness of the hydraulic lift is mainly controlled by the root vertical distribution, while the soil moisture levels at which hydraulic lift is most effective is dictated by soil hydraulic properties and surrogates for atmospheric water vapor demand.

Citation: Siqueira, M., G. Katul, and A. Porporato (2008), Onset of water stress, hysteresis in plant conductance, and hydraulic lift: Scaling soil water dynamics from millimeters to meters, *Water Resour. Res.*, *44*, W01432, doi:10.1029/2007WR006094.

1. Introduction

[2] Recent studies on the acceleration of the global hydrologic cycle [*Gedney et al.*, 2006], increases in the continental runoff [*Milly et al.*, 2005], and feedbacks to boundary layer processes [*Koster et al.*, 2004] are renewing interest in soil moisture dynamics and its controls on soil plant hydrodynamics at multiple scales. Specifically, plant transpiration is highly coupled with soil moisture state under water-limited conditions. Roots are responsible for harvesting most of the soil water, which then flows within the plant vascular system up to the leaves where it then evaporates from the stomatal pores. Thus it is not surprising that root water uptake is an active research subject within a wide range of scientific communities including hydrology, ecology, meteorology, and soil and crop sciences [*Feddes et al.*, 2001; *Hopmans*, 2006; *Laio et al.*, 2006; *Lee et al.*, 2005; *Tuzet et al.*, 2003; *Vrugt et al.*, 2001].

[3] Even though relatively little is known on how root anatomy and biochemistry regulate water flow [*Steudle*, 2000], a large number of conceptual and detailed representations have been proposed and used [*Li et al.*, 1999; *Vrugt et al.*, 2001]. Usually, water extraction by roots is simply modeled as a sink term added to Richards' equation, which governs the Darcy-scale water movement in the soil [*Vrugt et al.*, 2001]. This sink function must be dimensionally consistent with the corresponding form of Richards' equation (zero-dimensional (0-D), 1-, 2- or 3-D, 0-D being a bucket model) and be expressed as a function of local state variables such as soil moisture and solute concentration, and root density distribution.

[4] Accounting for the mechanisms responsible for the temporal dynamics of water stress within the soil-plant system is now central to the description of carbon uptake and its sequestration at interannual and longer timescales [*Siqueira et al.*, 2006]. It is generally accepted that plants regulate water use hydraulically through stomatal response to water pressure [*Tuzet et al.*, 2003], and/or biochemically, through stomatal response to abscisic acid hormone [*Davies and Zhang*, 1991; *Tardieu et al.*, 1992]. In addition, not without controversy, hydraulic lift (or hydraulic redistribution), which refers to the transport of water through the roots from wetter into dryer soil areas, is supposedly a mechanism that can facilitate water movement through the soil-plant-atmosphere system, delaying the onset of water stress [*Brooks et al.*, 2002; *Burgess et al.*, 1998; *Caldwell et al.*, 1998; *Dawson*, 1993; *Emerman and Dawson*, 1996; *Mendel et al.*, 2002; *Williams et al.*, 1993]. Evidence of hydraulic lift have been reported for shrub, grasses and tree species, and for temperate, tropical and desert ecosystems [*Caldwell et al.*, 1998; *Emerman and Dawson*, 1996; *Oliveira et al.*, 2005a, 2005b; *Yoder and Nowak*, 1999]. Very few root water uptake models account for hydraulic lift in their formulations, but recognition that such a mechanism may play a major role in the hydrologic cycle at scales much larger than plants is refocusing research efforts on the basic mechanisms enhancing hydraulic lift.

[5] *Lee et al.* [2005] included hydraulic lift through an empirical function that relates hydraulic lift to soil water potential in a regional atmospheric model and reported a significant increase in evapotranspiration and photosynthesis for the Amazon tropical forest if hydraulic lift is

[1]Nicholas School of the Environment and Earth Sciences, Duke University, Durham, North Carolina, USA.
[2]Departamento de Engenharia Mecânica, Universidade de Brasília, Brasilia, Brazil.
[3]Department of Civil and Environmental Engineering, Pratt School of Engineering, Duke University, Durham, North Carolina, USA.

Copyright 2008 by the American Geophysical Union.
0043-1397/08/2007WR006094$09.00

accounted for. *Mendel et al.* [2002] developed a root water uptake model that mechanistically resolves hydraulic lift. They confirmed through numerical simulations the general view that vegetation benefits from hydraulic lift in coping with water limitations suggesting perhaps that hydraulic lift may be a plant strategy. They also provided some evidence that this lift is hydraulic as opposed to osmotic.

[6] In solving Richards' equation, the presence of a rooting system profoundly changes the soil moisture dynamics. Root water uptake induces a radial flow toward rootlets [*Mendel et al.*, 2002]; but the overall rooting depth also interacts with a larger-scale soil moisture variations. Layers populated by roots experience lower soil moisture during a drying cycle thereby inducing upward flow from the deeper soil layers. Hence, at minimum, two flow patterns simultaneously occur at different length scales; the first is at scales comparable to the root zone depth (on the order of meters) and the second at length scales inversely related to root densities (on the order of millimeters). These two spatial scales are referred to as macroscale and mesoscale, respectively [*Mendel et al.*, 2002]. There are numerous fine-scale (microscale) processes often entirely ignored within the Darcian scale and are not considered here though their importance remains an open research question. Recognizing that both length scales are important in root water uptake, the macroscale impacting mean soil moisture states at longer timescales and the mesoscale capturing the maximum values of suction and daily hysteresis in root water uptake, these two flow patterns have been traditionally modeled independently without any attempt to couple them [*Guswa et al.*, 2004; *Mendel et al.*, 2002; *Puma et al.*, 2005; *Sperry et al.*, 1998; *Tuzet et al.*, 2003].

[7] Hence our main objective is to explore numerically this interplay between soil moisture redistribution, the vertical structure of the rooting system, soil type, and the role of hydraulic lift in mitigating plant water stress. In the numerical model, we make use of the scale separation between the macroscale (primarily vertical) and the mesoscale (primarily radial) flow patterns described above. The model solves each of them independently at very fine time steps and then recouples them through a simplified homogenization technique in space. Although there is no particular reason for this multidirectional grid approach not to be extended in two- or three-dimensional macroscale domains, computational demands would be prohibitive for long-timescale simulations relevant to ecosystem dynamics. Furthermore, the soil and root hydraulic properties are rarely known in two or three dimensions. For these reasons, a one-dimensional vertical macroscale approximation is used here for illustration. It is envisaged that these detailed model simulations can provide simplified scaling relationships describing what combinations of root distribution, soil types, and climatic conditions may promote hydraulic lift.

2. Theory

2.1. Model Description

[8] Water movement through the soil system is governed by Richards' equation [*Richards*, 1931]:

$$\frac{\partial \theta}{\partial t} = \nabla[K\nabla(\psi - z)], \tag{1}$$

where θ [m^3 m^{-3}] is the soil water content, t [s] is time, K [m s^{-1}] is hydraulic conductivity, ψ [m] is soil water potential, and z [m] is the vertical coordinate system. The variables θ, ψ, and K are related through the soil water retention and hydraulic conductivity functions,

$$\frac{\psi}{\psi_e} = \left(\frac{\theta}{\theta_s}\right)^{-b} \tag{2a}$$

$$\frac{K}{K_s} = \left(\frac{\theta}{\theta_s}\right)^{2b+3}, \tag{2b}$$

where θ_s [m^3 m^{-3}], ψ_e [m] and K_s [m s^{-1}] are saturation water content, air entry water potential and saturated hydraulic conductivity, respectively, and b is an empirical parameter [*Campbell*, 1985].

[9] Upon applying Kirchhoff integral transformation to ψ [*Campbell*, 1985; *Redinger et al.*, 1984] to define a "matric water potential" ϕ [m^2 s^{-1}], the second-order term in equation (1) can be linearized by writing ϕ as the driving force, given by

$$\frac{\partial \theta}{\partial t} = \nabla^2\phi - \frac{\partial K}{\partial z}. \tag{3}$$

Making use of the scale separation highlighted before and assuming horizontal homogeneity in root distribution, equation (3) can be approximated by a system of two coupled differential equations, one for the radial water flow in the vicinity of the root and a second describing the bulk water vertical motion,

$$\frac{\partial \theta(r,z,t)}{\partial t} = \frac{1}{r}\frac{\partial}{\partial r}\left(r\frac{\partial \phi(r,z,t)}{\partial r}\right) - \frac{\partial q_z(z,t)}{\partial z} - E_s(z,t) \tag{4a}$$

$$\frac{\partial q_z(z,t)}{\partial z} = \frac{\partial^2 \overline{\phi}\left(\overline{\theta}(z,t)\right)}{\partial z^2} - \frac{\partial \overline{K}\left(\overline{\theta}(z,t)\right)}{\partial z}, \tag{4b}$$

where q_z [m s^{-1}] is a vertical flow rate and the overbar represents a layer-averaged value. Here we introduced a sink term E_s [s^{-1}] to account for soil water evaporation. The coupling variable q_z is estimated from a space average of the matric water potential and hydraulic conductivity. For consistency, these averages should be estimated using functional relationships given by equation (2), where $\overline{\theta}$ is the mean value of the soil moisture at each z location and is given by

$$\overline{\theta}(z,t) = \int_{r_r}^{R(z)} \theta(r,z,t)2\pi r\lambda(z)dr, \tag{5}$$

where λ [m m^{-3}] is root length density, r_r [m] is root radius and R [m] is the size of radial domain. In equation (5) it is assumed that λ is uniformly distributed horizontally and R is halfway distance between rootlets. A schematic diagram of the model framework is shown in Figure 1. The model estimates soil moisture distribution by dividing the vertical domain into layers, and solving equation (4a) from r_r to R for each individual layer. To solve equation (4a), boundary conditions

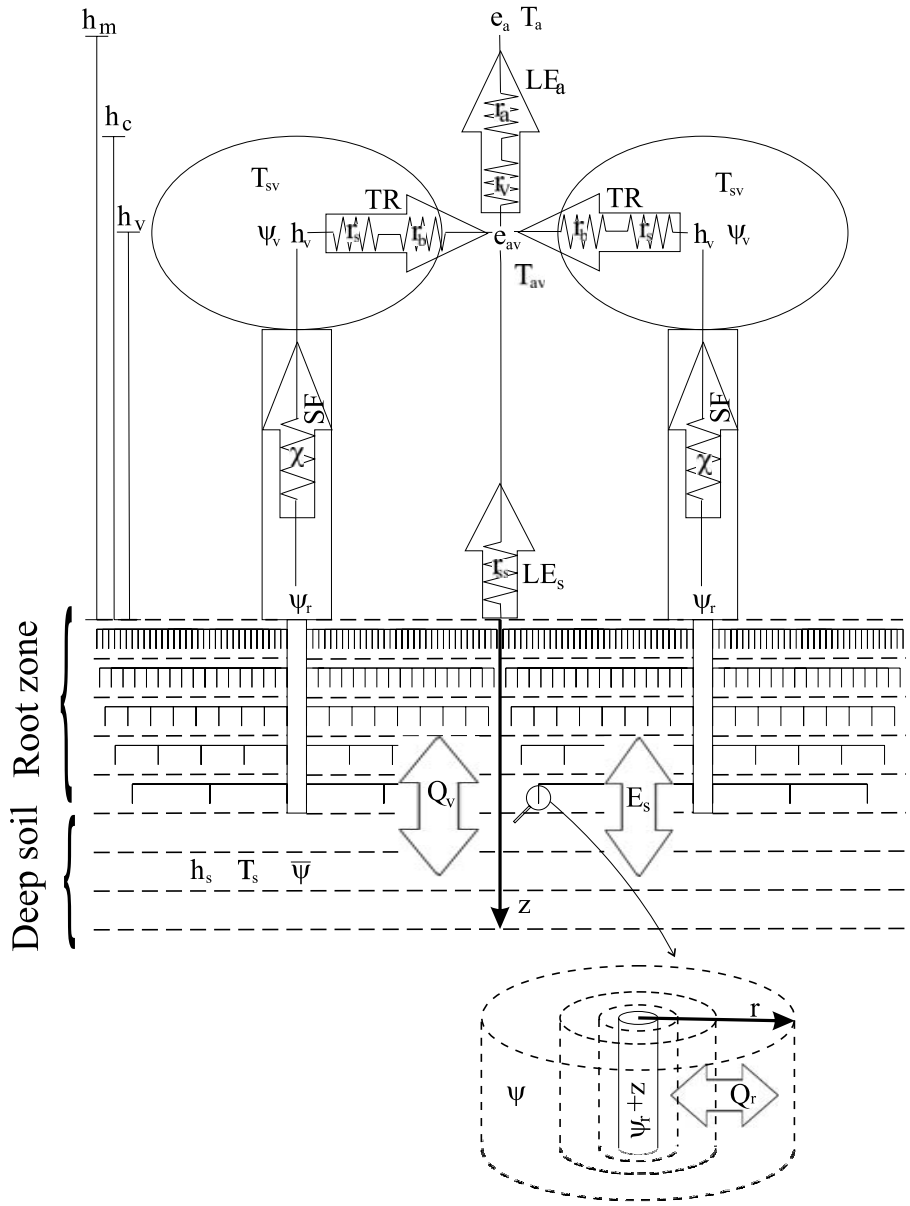

Figure 1. Schematic representation of the water flow components in the model. Q_v and Q_r represent the vertical and radial fluxes, respectively, obtained from Richards' equation; SF and TR are sap flow and transpiration (assumed equal in the absence of capacitance); E_v is volumetric soil water evaporation; LE_s is water vapor flux from the soil; and LE_a is evapotranspiration. The state variables are ψ (mesoscale soil water potential), $\overline{\psi}$ (macroscale soil water potential), ψ_r (root pressure), ψ_v (leaf pressure), T_s (soil temperature), T_{sv} (leaf temperature), T_{av} (canopy air temperature), T_a (air temperature), h_s (soil fractional relative humidity), h_v (leaf fractional relative humidity), e_{av} (canopy air water vapor pressure), and e_a (air water vapor pressure). The resistors include χ (leaf-specific root to shoot resistance), r_s (stomatal resistance), r_b (boundary layer resistance), r_{ss} (soil to canopy air aerodynamic resistance), and r_a and r_v (canopy air to air aerodynamic resistance). The heights are h_m (measurement height), h_c (canopy height), and h_v (mean canopy source/sink height).

(hereafter referred to as BC) must be prescribed. At $r = R$, symmetry requires a zero flux BC. At $r = r_r$, the BC is the root water uptake occurring at the interface between the root and soil. When root water uptake is hydraulically controlled, it is given by

$$q_r(z) = K_r[\psi_r - z - \psi(r_r, z)], \tag{6}$$

where K_r [s^{-1}] is a root membrane permeability, and ψ_r [m] is the root pressure referenced to ground level.

[10] Transpiration TR [m s^{-1}] is assumed to be equal to the sap flow (no capacitance) and is given by [*Tuzet et al.*, 2003]

$$TR = \frac{\psi_r - \psi_v}{\chi} = \frac{M_w}{\rho_w R_g}\frac{1}{r_s + r_b}\left(\frac{h_v e_{sv}}{T_{sv}} - \frac{e_{av}}{T_{av}}\right), \tag{7}$$

where ψ_v [m] is bulk leaf water potential, χ [s] root to shoot plant hydraulic resistance, R_g [J mol^{-1} K^{-1}] is the universal gas constant, M_w [kg mol^{-1}] and ρ_w [kg m^{-3}] are the water molecular weight and density, respectively, T_{sv} [K] and e_{sv} [Pa] are leaf temperature and saturation vapor pressure at leaf temperature, respectively, and T_{av} [K] and e_{av} [Pa] are temperature and vapor pressure of the air surrounding the leaves, $h_v(= \exp(M_w\ \psi_v\ g/R_g/T_{sv}))$ is fractional relative humidity in the leaf intercellular spaces, g [m s^{-2}] is gravity and r_b [s m^{-1}] and r_s [s m^{-1}] are bulk boundary layer and stomatal resistance, respectively.

[11] Stomatal response to a drying soil regulates transpiration losses by chemical and/or hydraulic signaling from root to leaf as root water potential becomes more negative [*Davies and Zhang*, 1991; *Jones and Sutherland*, 1991; *Sperry*, 2000; *Tardieu and Davies*, 1993; *Tardieu et al.*, 1992; *Tyree and Sperry*, 1988]. A logistic function is often used to describe the stomatal sensitivity (or vulnerability) to leaf water potential, given by [*Tuzet et al.*, 2003]

$$g_s = \frac{\beta}{r_s} = g_0 + (g_{\max} - g_0) f_\psi \tag{8a}$$

$$f_\psi = \frac{1 + \exp\left[s_f \psi_f\right]}{1 + \exp\left[s_f\left(\psi_f - \psi_v\right)\right]}, \tag{8b}$$

where g_s [mol m^{-2} s^{-1}] is stomatal conductance, g_0 [mol m^{-2} s^{-1}] and $g_{\max}$ [mol m^{-2} s^{-1}] are residual and maximum stomatal conductance, respectively, β [mol m^{-3}]$(= P_a/R_g T_a)$ is a conversion factor from molar units to physical resistance, P_a [Pa] and T_a [K] are atmospheric pressure and temperature, respectively. The f_ψ is a reduction function with empirically determined sensitivity parameter s_f and reference potential ψ_f [m]. This reduction function makes stomatal conductance relatively insensitive to ψ_v when ψ_v is close to zero but as ψ_v approaches ψ_f, it rapidly decreases.

[12] To solve equation (4b), BCs must also be specified. The top boundary condition is zero flux unless there is infiltration (not considered here). At the lower domain limit, drainage is estimated by extrapolating the matric potential. For this estimate to be realistic, the soil domain must be extended well beyond the root zone otherwise differential water uptake creates water potential gradients unrealistic for root free soil. This may be avoided by extending the root zone and assigning very small root density values beyond the actual rooting depth. However, this approach would require unnecessary radial flow calculations thereby increasing the computational time. To overcome this, we model water movement in the soil in two distinct zones - a root zone and a deep soil layer (root free). For the root zone, equations (4), and (5) are employed. For the deep soil, equations (4a) and (5) can be expressed as

$$\frac{\partial \bar{\theta}(z,t)}{\partial t} = \frac{\partial^2 \bar{\phi}(z,t)}{\partial z^2} - \frac{\partial \bar{K}(z,t)}{\partial z} - E_s(z,t). \tag{9}$$

Evaporation required here for solving equations (4a) and (9) is modeled using a simple water vapor diffusion equation with fractional relative humidity as the driving gradient. Thus evaporation depends on soil temperature T_s and $\overline{\psi}$. Soil temperature is computed by solving the heat flow equation. The coupling between transpiration and atmospheric evaporative demand (see equation (7)) introduced two new unknowns: T_{sv} and T_{av}. Additional equations necessary to "close" this problem are provided by the energy balances for leaf and canopy air and a radiation partitioning model (see appendix A).

[13] The differential equations are discretized using a control volume approach with central differencing schemes for spatial derivatives and implicit scheme for time derivatives. An integrated numerical solution for ψ, ψ_r, ψ_v, T_s, T_{sv} and T_{av} is obtained using an iterative Newton-Raphson method.

2.2. Model Assumptions and Limitations

[14] The model assumes that root absorption is driven by pressure differences between root-soil interface and root xylem tissue. For high soil moisture states, these differences are small and root absorption is known to be mostly controlled by osmotic processes (neglected here). However, as the soil dries, the pressure differences builds up and root uptake becomes hydraulically controlled [*Niklas*, 1992].

[15] Additionally, contrary to other studies [*Mendel et al.*, 2002], the model neglects pressure losses within root xylem. Order-of-magnitude arguments [*Lafolie et al.*, 1991] show that the root pressure is hydrostatically distributed and simply adjusts to maintain the transpiration demand, the latter being driven by photosynthesis. This argument simplifies modeling water flow inside the rooting system assuming pressure losses within the roots are small compared to the pressure drop in the soil and across the root-soil interface. This assumption becomes more realistic as the soil dries given that the soil hydraulic conductivity decreases exponentially while root xylem conductivity remains constant (near its saturated value). The pressure drop in the root xylem at different depths because of differences in root xylem path lengths for nonhomogenous vertical root distribution can be partially accounted for in the model by considering K_r as bulk resistance and variable with depth.

[16] As in the work by *Tuzet et al.* [2003], the model assumes horizontal homogeneity for the root area distribution. This assumption is reasonable if the macrovariations in soil moisture are primarily one-dimensional (i.e., vertical gradients are much larger than planar gradients). If the macroscale gradients are not primarily one-dimensional (not accounted for here), then macroscale horizontal flow is likely to be significant requiring a full 3-D solution of Richards' equation or axisymmetric solution [*Mendel et al.*, 2002]. The implications are that hydraulic lift is no longer a "lift" from deeper soil layers and can be modulated by lateral macroflow. For sparser and less homogeneous canopies, the one-dimensional macroflow assumption may not be reasonable. In addition, gravity is neglected in the radial domain, which makes rootlet orientation immaterial. The higher gradients and faster dynamics in the radial direction justify this assumption as we show later.

[17] Furthermore, for a highly dense rooting system, the radial domain could be of sizes (<1 mm) that challenges the applicability of Darcy's law (and consequently Richards' equation). Fundamentally, the representative elementary volume could be too small to treat the soil pores as

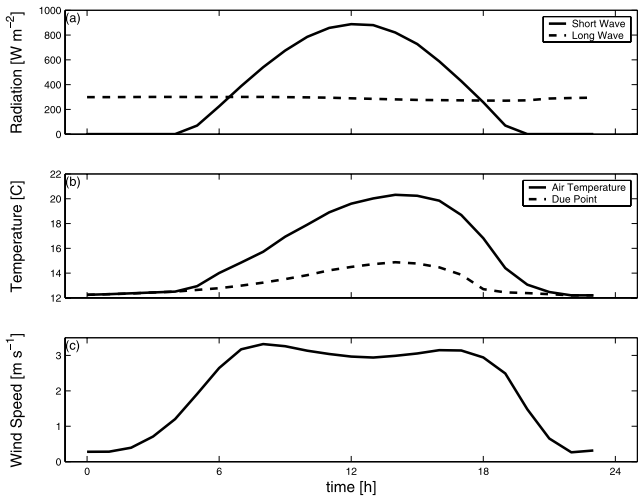

Figure 2. Daily variations of (a) incoming radiation, (b) air temperature and due point, and (c) wind speed.

statistically homogeneous, yet too large to consider computationally the full Navier-Stokes equations on each pore. However, in these cases, the formulation may be robust to the precise law governing water movement to the roots. The reason for this robustness is that for such short distances, the physical law is just providing an estimate of the travel time between the water source and the root. Given that these travel times are much shorter than the macrochanges in soil moisture, the approach here simply interprets the change in soil moisture due to root uptake as occurring almost instantaneously. This near instantaneous approximation must be referenced to other timescales responsible for changes in soil moisture. With radial distances that small, water molecules within this radial domain between adjacent roots arrive at the root surface much faster than any other timescale of changes in water movement in the soil-root system. It is unlikely that moisture differences across radial domain will play a significant role in the total water to be extracted from this layer by the roots (they may change the precise value of the travel time). Nevertheless, because the vertical water flow between different soil layers is through layer-averaged soil moisture, the model framework could be revised by applying a different (empirical) model for highly dense layers and retain the Darcy-Richards' model for deeper and less dense (in terms of roots) soil layers where radial soil distribution might be important for the dynamics of water stress experienced by the vegetation. However, this revision is not likely to yield any major improvement given the separation in timescales.

3. Results

[18] The interplay between soil moisture redistribution, the vertical structure of the rooting system, and the role of hydraulic lift in mitigating plant water stress are explored via a number of model runs. To compare with hydraulic models that only resolve the radial component, the same atmospheric drivers (assumed periodic on a daily timescale) for transpiration (Figure 2), plant physiological and hydraulic characteristics for all simulations from *Tuzet et al.* [2003] were used, except for the root membrane permeability, K_r, which was absent in their model (Table 1).

Table 1. Parameters for the Vegetation and Stomatal Conductance Model Used in All Model Runs[a]

Vegetation	Value	Units
Leaf area index LAI	3	
Canopy height h_c	0.8	m
Average leaf width l_c	1×10^{-2}	m
Canopy mixing length l	0.2	m
Root depth Z_R	1	m
Root radius r_r	1×10^{-4}	m
Root length density λ	4×10^{3}	m m^{-3}
Plant hydraulic resistance χ	1.06×10^{9}	s
High root permeability K_r	1×10^{-8}	s^{-1}
Low root permeability K_r	1×10^{-9}	s^{-1}
Stomatal conductance		
Residual conductance g_0	4.8×10^{-4}	mol m^{-2} s^{-1}
Maximal conductance g_{max}	0.56	mol m^{-2} s^{-1}
s_f	3.14×10^{-2}	m^{-1}
ψ_f	−193	m

[a]Runs use the same values used by *Tuzet et al.* [2003]. Note the two values of root permeability used to simulate high and low hydraulic lift scenarios.

3.1. Numerical Experiments

[19] Three different root vertical distributions with equal rooting length density were studied (see Table 1) as shown in Figure 3. These distributions span a wide range of plausible rooting profiles [*Hao et al.*, 2005] varying from the simplest case of a constant root density [*Tuzet et al.*, 2003] to a power law root distribution often reported in field studies [*Jackson et al.*, 1996]. Three different soil types were also explored: a sandy loam, a silt loam, and a loam (see Table 2 for hydraulic properties). For consistency, soil properties for different soil types were assumed the same as reported by *Tuzet et al.* [2003]. Since the ability of the rooting system to uplift water is controlled by K_r, two K_r values were used (see Table 1): one promotes a "high hydraulic lift," which is about the highest value reported in other studies [*Mendel et al.*, 2002], and another promotes "low hydraulic lift," set at 1 order of magnitude lower. To isolate the effects of hydraulic lift, these reductions in K_r

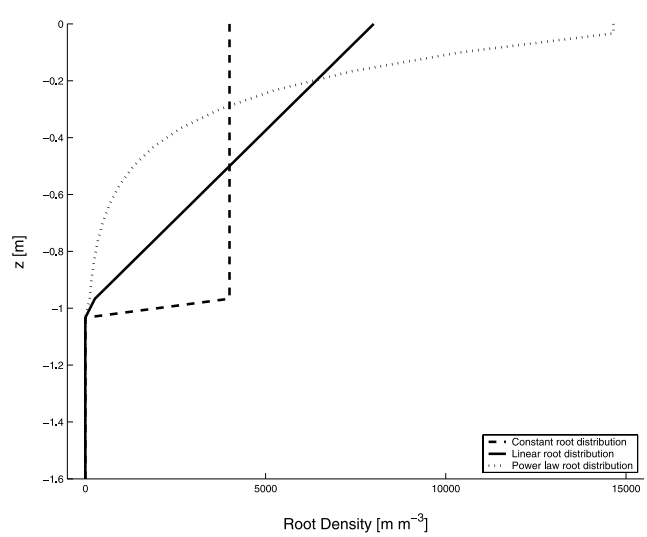

Figure 3. Three canonical rooting profiles: constant, linear, and power law. All three have identical total root length.

Table 2. Soil Hydraulic Properties for the Three Soil Types[a]

Parameter	Soil Type		
	Sandy Loam	Silt Loam	Loam
b	3.31	4.38	6.58
Saturation soil water content θ_s	0.4	0.4	0.4
Air entry water potential ψ_e, m	−0.093	−0.161	−0.192
Saturated water conductivity K_s, m s^{-1}	9.39×10^{-6}	2.14×10^{-6}	2.24×10^{-6}

[a]Soil types are the same as those used by *Tuzet et al.* [2003].

were followed by an increase in plant hydraulic resistance such that the overall resistance from the soil to the leaf was kept identical across K_r simulations. For this reason, reductions in K_r beyond this minimum would require an unrealistic reduction in plant hydraulic resistance.

[20] The model runs include 18 combinations of soil types (3), root vertical distributions (3), and root permeability (2). To avoid arbitrary prescription of soil moisture vertical distribution, which is not independent of soil properties and root density profiles, initial conditions for all simulations were identically set at near saturation to permit comparisons across runs. Excess water from field capacity drains in the first few days of the simulation, and drainage has a minor impact beyond this point. For illustration, we show results for the silt loam soil type when discussing different root distributions and K_r, and the linear root distribution when contrasting different soil types and K_r. The choice of a linear root profile and silt-loam soil as baselines for comparison is not intended to be baselines for "field" realism. They are chosen as intermediate representation between the end-members for both soil type and complexity in root vertical distribution. In the discussion section, we propose a simplified scaling argument that collapses the importance of hydraulic lift in all 18 simulations.

3.2. Indirect Verification of the Hydraulic Lift

[21] Experimentally, daily hydraulically uplifted water (HLW [m d^{-1}], defined as the total amount of water released by the roots, positive sources only, over the course of a day) of 102 ± 54 [L d^{-1}] was estimated for a sugar maple tree that transpired 400–475 [L d^{-1}] [*Emerman and Dawson*, 1996]. The rooting system of this tree extended 5 m radially, which would yield an amount of $(1.30 \pm 0.69) \times 10^{-3}$ [m d^{-1}] for a transpiration rate of 5.1×10^{-3} to 6.5×10^{-3} [m d^{-1}]. Potential daily transpiration under the environmental condition used in our calculations was 3.06×10^{-3} [m d^{-1}]. Furthermore, our maximum HLW calculated values were 1.14×10^{-3} and 0.80×10^{-3} [m d^{-1}] for high and low hydraulic lift respectively, or 37% and 25% of potential transpiration, which agree with these measurements [*Emerman and Dawson*, 1996]. The model calculations by *Mendel et al.* [2002] reported a HLW of 172 [m d^{-1}] (2.19×10^{-3} [m d^{-1}]) for this same sugar maple tree. They attributed the overestimation to absence of the mesoscale effects in their model, which suggests that the model presented here recovers the proper magnitude of the "mesoscale" effect they anticipated.

[22] To evaluate the model realism in capturing the hydraulic lift contribution to transpiration, Figure 4a presents the time series of calculated HLW for the linear root distribution profile and for a silt loam soil using both the high and low K_r values. Figure 4b shows the centroid of root water uptake vertical distribution on a daily timescale for the same model runs as in Figure 4a.

[23] Following the rapid drainage phase, the contribution of HLW progressively increased as the vertical water potential gradients build up (see Figure 4a). HLW reached a maximum and started to decrease as the soil dries because now the lower conductivity makes it difficult for water to populate drier spots closer to the root-soil interface (see also Figure 5a).

[24] Additionally, because of its vertical resolution of soil moisture, the model allows the root system to extract water where it is available, a behavior known as compensatory uptake [*Skaggs et al.*, 2006]. Figure 4b suggests that hydraulic lift enhances the ability to perform this compensatory uptake.

[25] Figure 5a shows the water uptake profiles from linearly distributed root and a silt loam soil with high K_r at different times of day and for different days as the drying cycle progresses. The days were chosen to represent the minimum HLW at the beginning of the simulation period (near saturation), the day of maximum HLW and a time of HLW with water stress. The times were 0000 (midnight) when hydraulic lift is active and 1200 (noon) when transpiration is dominant. Figure 5b shows the pressure distribution at the root-soil interface along with the root pressure, assumed hydrostatically distributed. Also included in Figure 5b is the layer-averaged soil pressure. The pressure profiles shown are for day 100 into the simulation, the day of maximum HLW.

[26] At the early stages, most of the water uptake comes from the topsoil layers, given the water availability and higher root density. As the simulation progresses, water

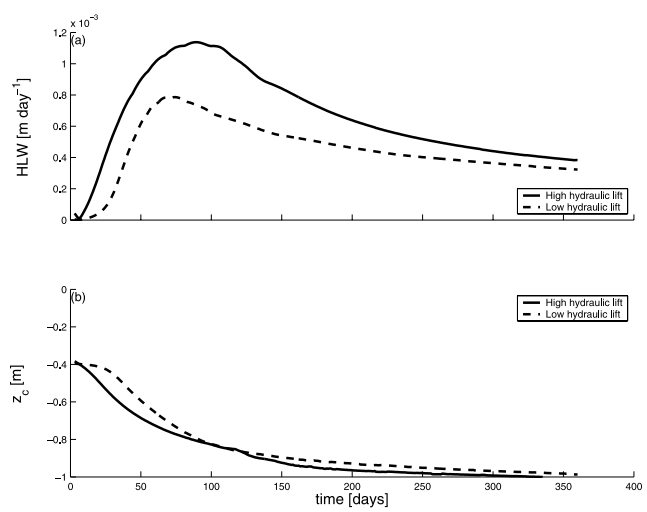

Figure 4. (a) Modeled hydraulically lifted water (HLW) for linearly distributed roots in a silt loam soil as a function of time (t). The two lines represent HLW for high and low K_r values. (b) Centroid of root water uptake vertical distribution at daily timescale as in Figure 4a; the two lines are for different K_r.

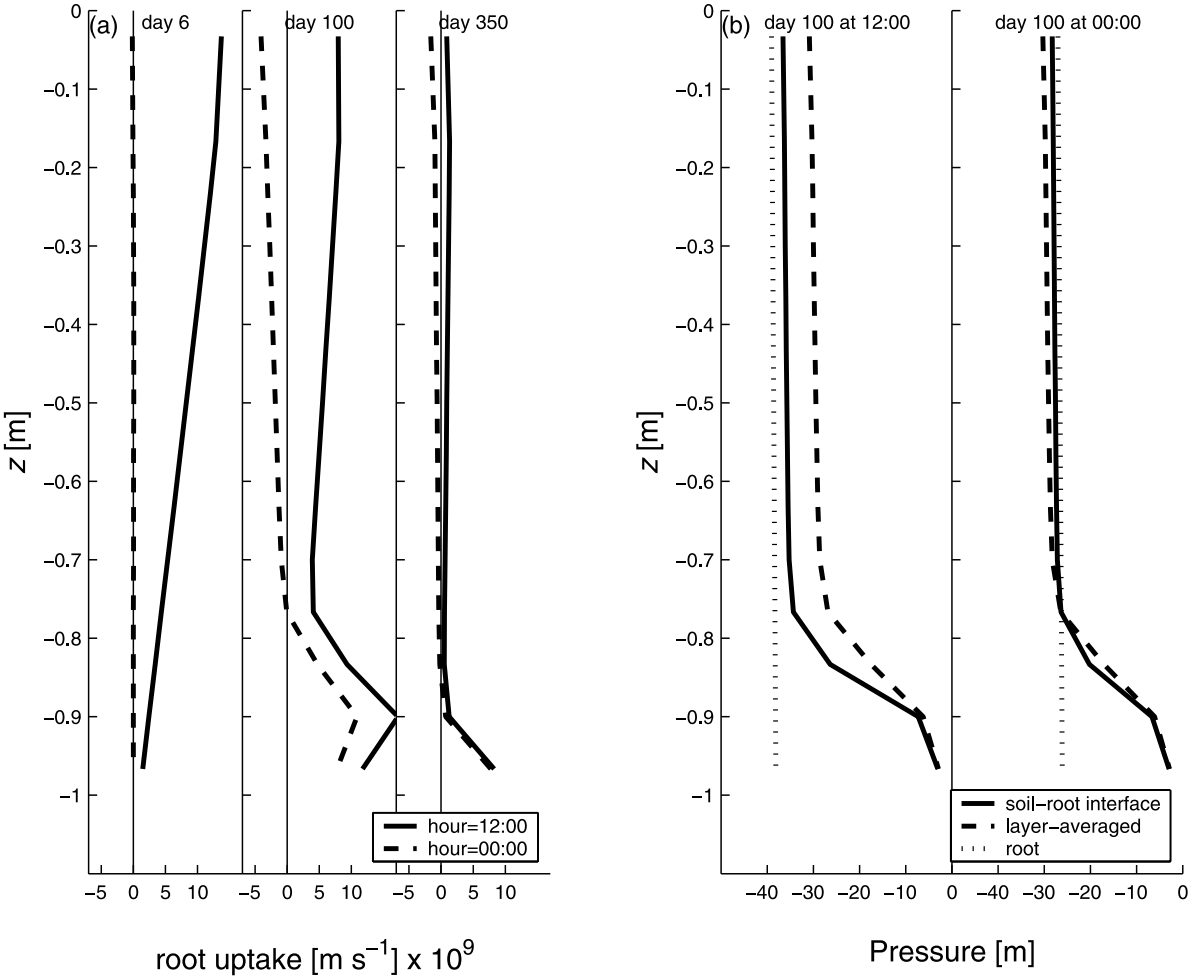

Figure 5. (a) Modeled root water uptake profiles at noon (solid lines) and midnight (dashed lines) for different days and for the linearly distributed roots in a silt loam soil and high K_r. (b) Vertical pressure profiles of the root-soil interface and root system (hydrostatically distributed) along with layer-averaged soil pressure. The profiles plotted are for period of maximum HLW (day 100) for different times during this day.

uptake in the deeper layers becomes more important as it contributes to transpiration and to hydraulic lift for non-transpiring (nighttime) periods. At the end, most of the water is coming from the deeper layers, given that the uptake from the top layers seems to be hydraulically lifted water from the previous night. Pressure distribution on day 100, reveals the interesting dynamics that leads to hydraulic lift (Figure 5b). During day time, root pressure required to maintain transpiration is lower then root-soil interface pressure at all depths. When transpiration seizes, root pressure adjust to zero transpiration and falls in between root-soil interface pressure distribution, setting the stage for hydraulic lift.

[27] With regards to model assumptions (see section 2.2), notice the comparable pressure differences for radial (represented in Figure 5b by the difference between layer-averaged and soil-root interface pressures) and vertical directions. While these pressure differences are comparable, they occur over very different length scales (of order millimeters for radial and meters for vertical). Hence the pressure gradients in the radial direction are about 3 orders of magnitude larger than the vertical gradients (and justifying the absence of gravitational effects in the radial formulation). Also notice that the radial gradients switch signs between day and night characterizing a faster dynamics of radial flow. This radial drying processes and the concomitant reduction in hydraulic conductivity was referred earlier to as mesoscale effect [*Mendel et al.*, 2002]. The model of Mendel and coworkers partially accounted for this mechanism by introducing an empirical extraction function that is linearly related to soil moisture. This is a reasonable assumption but clearly will not allow for daily hysteresis in stomatal conductance as suggested by others [*Eamus et al.*, 2001; *Grant et al.*, 1995; *Prior et al.*, 1997], which is a direct consequence of "radial" water flow dynamics [*Tuzet et al.*, 2003] (accounted for in the present model). Hence the approach used here is a "compromise" between the model of *Tuzet et al.* [2003] (mainly radial and detailed leaf hydraulics) and the more detailed soil-root system model of *Mendel et al.* [2002].

3.3. Effect of Hydraulic Lift on Soil-Plant Interactions

[28] In Figure 6, the relationship between transpiration and vertically integrated soil water content in the root zone

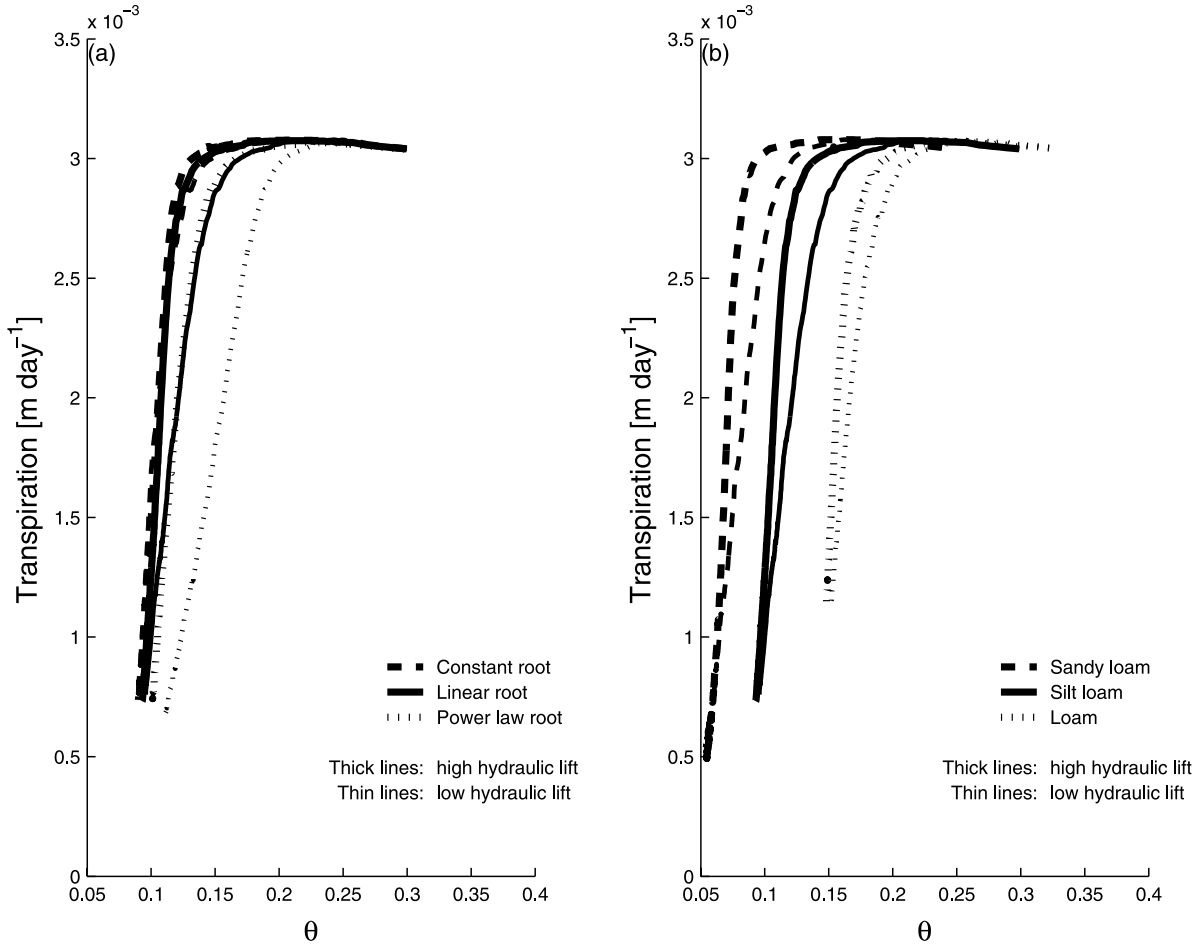

Figure 6. Variations of transpiration with vertically averaged root zone soil moisture for high and low values of K_r: (a) different root distribution for silt loam soil type and (b) same results for different soil types for linearly distributed roots.

is shown. Interestingly, vegetation with homogeneous vertical root distribution sustains transpiration at lower soil moisture content (see Figure 6a). Compared to water redistribution by "soil physics" alone, hydraulic lift is highly efficient in redistributing water within the rooting volume. The small variation in root pressure (relative to the soil water pressure) results in nonlocal redistribution while water movement through soil pores in the absence of root uptake is exclusively dependent on local gradients in water potential. Naturally, the more asymmetric the rooting system is the more beneficial the hydraulic lift is in avoiding water stress as shown in Figure 6a. Furthermore, the model predicts that sandy soils can sustain transpiration for lower soil water states (Figure 6b) as expected. Similarly, hydraulic lift increased the ability of the soil-plant system to transpire water with drier soil water states for all three soil types considered here.

[29] Implications of this different loss function for the onset of water stress are explored in Figure 7. It clearly shows that hydraulic lift is responsible for delaying the onset of water stress for all cases, consistent with other findings [*Mendel et al.*, 2002]. Even though sandy soils can sustain higher rates of transpiration with lower soil saturation, loamy soils delay water stress onset because of higher field capacity (Figure 7b). In addition, loamy soils promote more hydraulic lift when compared to other soil types, as expected from a "mesoscale" effect.

[30] Additionally, an increase in asymmetry in rooting distribution shape also enhances hydraulic lift. Notice that the delay in water stress between high and low hydraulic lift due to different root distribution is comparable to the delay due to different soil types. Surprisingly, however, considerable water stress delay (in transpiration) was noted with a constant root distribution. Again, *Mendel et al.* [2002] reported similar findings with respect to HLW, which was weakly correlated with their vertical root distribution parameter. Two explanations are plausible: (1) the internal circulation by hydraulic lift is equally beneficial independent of the root distribution, or (2) water from wetter soils below the rooting zone are first transported to the rooting zone (via soil physics alone through Darcian flow), then hydraulically uplifted to shallower layers that are populated by more roots, where they again significantly contribute to transpiration during day time. The later mechanism benefits the constant root distribution more given the higher water potential gradients at the transition between the rooting system and the deeper soil layers. This soil water contribution from deeper soil layers overcompensates for the more beneficial redistribution role of hydraulic lift for asymmetric root distributions.

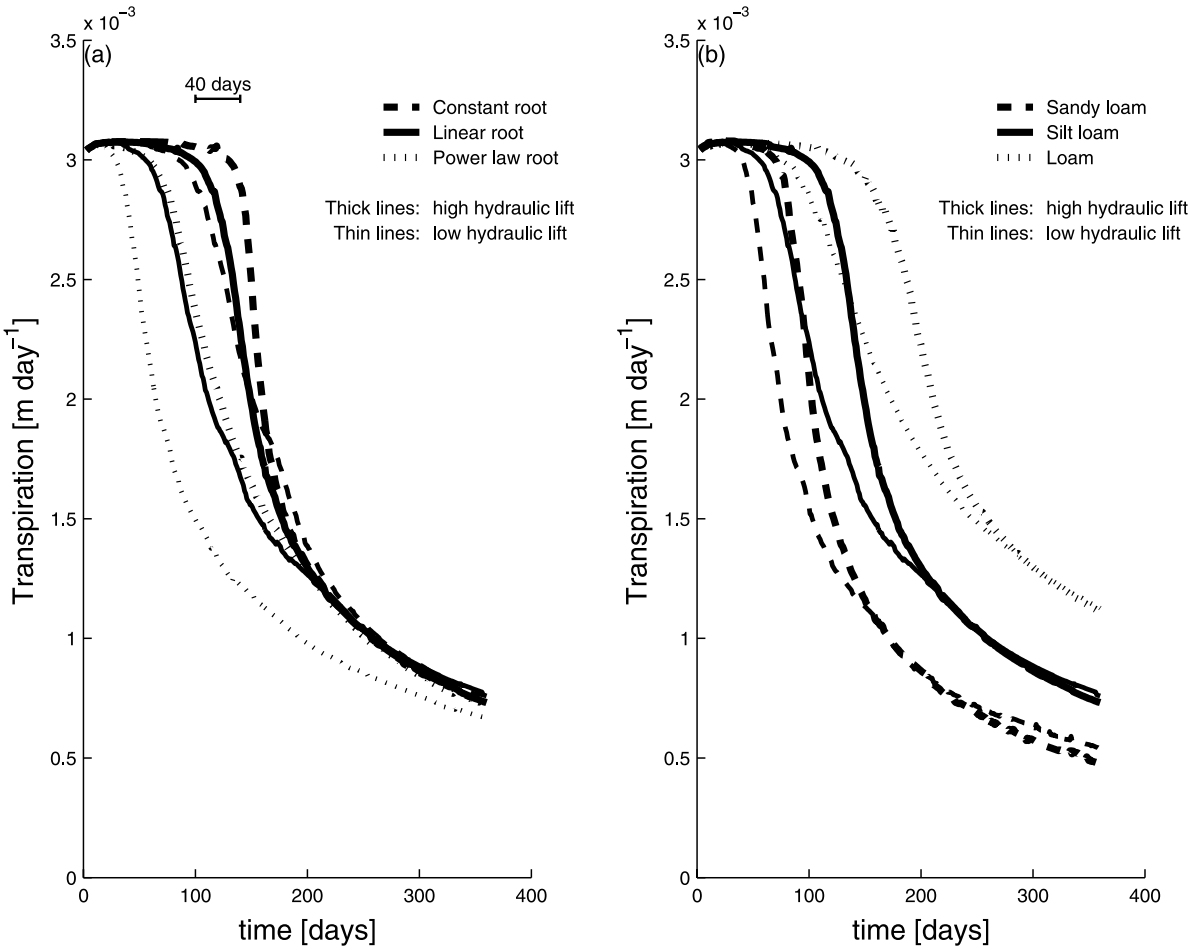

Figure 7. Transpiration as a function of time with high and low values of K_r: time variation of different root distributions for (a) silt loam soil type and (b) different soil types with linearly distributed roots.

[31] To explore these two possibilities further, daily values of water flux at the interface between the deep soil and root zone for the different root distributions in a silt loam soil type is shown in Figure 8. A large drainage occurs at early stages characterized by the negative flow in the first days of the simulation. After soil water state changes from fully saturated to close to field capacity, water starts moving up from deeper soil into rooting zone by soil physics alone (no root uptake). Figure 8 clearly shows higher flow rates for constant root distribution for high K_r. These results are highly suggestive that hydraulic lift and soil physics-based vertical transport synergistically act together so that the plant can cope with prolong droughts, provided that deep soil layers are sufficiently wet.

[32] Additional simulations (with high and low K_r) were also performed for a single soil layer (rooting zone only) with constant root distribution with no drainage allowed (zero flux lower boundary condition at the bottom of the vertical domain). These simulations were performed with vertical discretization and with a single node (vertical domain represented by just one element). For the latter, hydraulic lift is immaterial and the model reduces to the approach of *Tuzet et al.* [2003]. Results (not shown) of those simulations were indistinguishable further confirming the hypothesis that hydraulic lift and soil physics acting cooperatively. Hence, if no soil water is available to move up

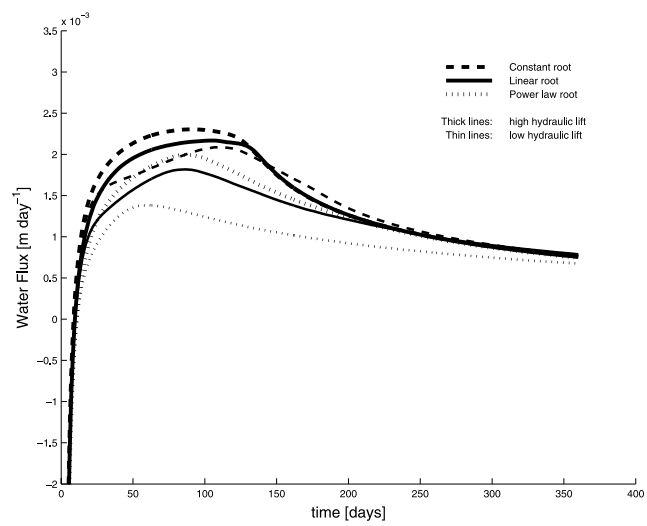

Figure 8. Daily water flux at the interface between the deep soil layer and root zone for different root distributions and for silt loam soil type. The sign convention is positive for upward flow and negative for downward flow. Note that drainage dominated the early phases and because of its large magnitude is only shown after 3 d of simulation.

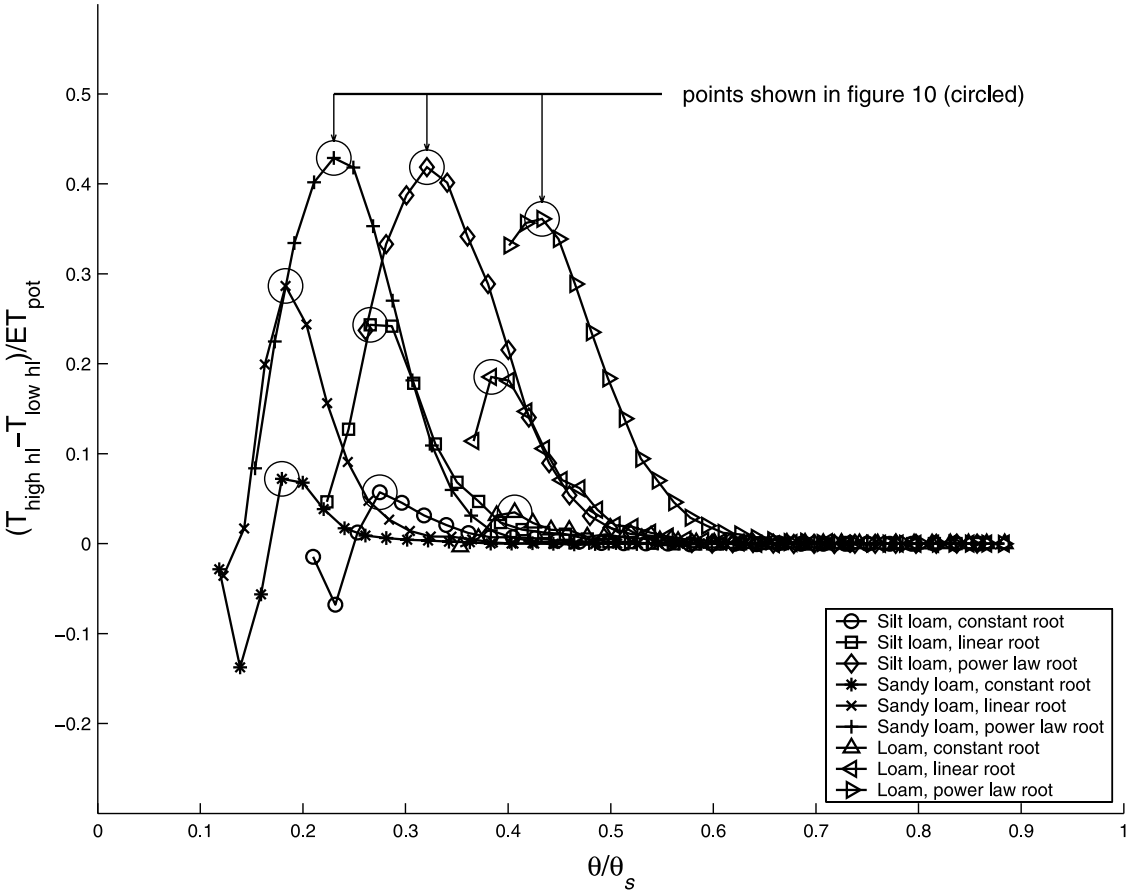

Figure 9. Difference between transpirations (normalized by potential evapotranspiration) with high and low values of K_r as a function of root zone-averaged soil moisture for all soil types and all root distribution. The circled points refer to values presented in Figure 10.

from the deeper soil system, and if the heterogeneity in the vertical distribution of root is not too strong, no significant gain is obtained by the vertical resolution of soil moisture, at least in terms of water stress experienced by plants. However, as mentioned before, typical vertical root distribution patterns follows a power law and drainage is expected in most cases making this situation uncommon.

4. Discussion

[33] The interplay between soil moisture redistribution, the vertical structure of the rooting system, soil type, and the role of hydraulic lift in mitigating plant water stress are explored here using a simplified scaling analysis applied to the results in Figure 9. Figure 9 presents the difference between high and low hydraulic lift transpiration rates as a function of soil saturation for all 18 simulations. It suggests that hydraulic lift may be characterized by two variables: (1) the maximum value of the difference between high and low K_r, which is a measure of hydraulic lift effectiveness, and (2) its concomitant soil moisture state. For the purpose of data analysis and experimental design, it is beneficial to find relationships between hydraulic lift and internal properties of the soil-root system. The internal controls on hydraulic lift are related to the soil's ability to redistribute water and the asymmetry of the root distribution. The latter is partially responsible for creating the departure from hydrostatic water potential profile and is the driver for this redistribution.

[34] Figure 10 shows the two characterizing hydraulic lift variables against the ratio of root distribution centroid and root depth (a measure of root asymmetry, Figure 10a) and against specific soil moisture capacity ($C = d\theta/d\psi$ [m], Figure 10b) normalized by root depth. This analysis suggests that hydraulic lift effectiveness is mainly controlled by root distribution. On the other hand, the soil moisture levels at which hydraulic lift is most effective is dictated by soil hydraulic properties.

[35] The dynamics of root water uptake and its relationship with soil type and root distribution is central to understanding the coupling between water cycle and water stress experienced by plants. The nonlinear interaction of evapotranspiration and intermittent precipitation distribution, followed by pulses of infiltration, must be accounted for the comprehension of the feedbacks between above and below-ground processes. In addition, estimation of vegetation response to shifts in precipitation regimes due to climate change and/or land use change requires models that preserve the dynamics of root water uptake such that water stress (timing and effect on transpiration) will be properly reproduced. Hence models that mechanistically integrate above and below ground process are needed to address these issues and the model presented here or simpler models

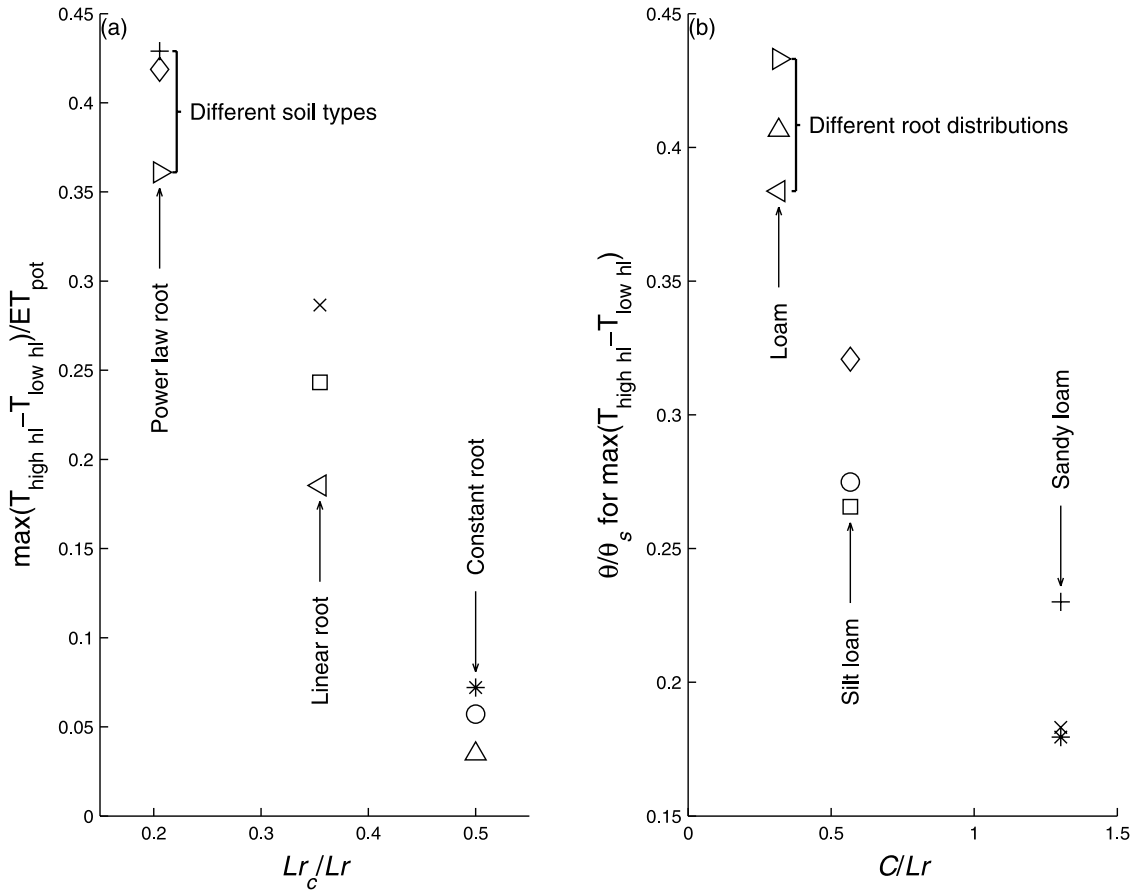

Figure 10. (a) Maximum values of transpiration difference with high and low values of K_r (normalized by potential evapotranspiration) as a function of the centroid of the root distribution (normalized by root depth). (b) Soil moisture levels at which those maxima occur as a function of specific soil moisture capacity C (also normalized by root depth).

that capture some features highlighted in this analysis would be a first step in this direction.

5. Summary and Conclusions

[36] The main objective here was to explore the interplay between soil moisture redistribution, the vertical structure of the rooting system, soil type, and the role of hydraulic lift in mitigating plant water stress. Making use of the scale separation between macroscale (primarily vertical) and mesoscale (primarily radial) flow patterns, a numerical model that solves each independently and couples them through a simplified horizontal averaging technique was proposed and used to address the main objective. The conclusions can be summarized as follows:

[37] 1. The newly proposed model was able to account for known features of root water uptake such as diurnal hysteresis of canopy conductance, water redistribution by roots (hydraulic lift) and downward shift of root uptake during drying cycles (compensatory uptake [*Skaggs et al.*, 2006]).

[38] 2. The root vertical distribution is, at least, as important as soil type in modeling water stress in water limited ecosystem.

[39] 3. The hydraulic lift could be significant and must be accounted for in models of water stress and its onset.

[40] More broadly, the scaling analysis on hydraulic lift effectiveness can guide field experiments as to some necessary conditions for its onset and maximum contribution. Last, the formulation proposed here has the added benefit in that it can be readily integrated with detailed aboveground plant-hydrodynamics models [*Bohrer et al.*, 2005; *Chuang et al.*, 2006] given its dependence on the plant water potential and the vulnerability curve. Such a combination can provide a simulation platform for the development of simplified models (e.g., vertically integrated column models) for root water uptake that can account for hydraulic lift contribution.

Appendix A: Energy Balance Model

[41] The aboveground energy balance used here is similar to the model of *Tuzet et al.* [2003]. For below ground, a diffusion equation for heat and water vapor in the soil is used. For completeness, a brief description of the model components is provided. The net radiation absorbed by foliage, Rn_v, and soil, Rn_s, are given by

$$Rn_v = (1 - a_v)SW[1 - \exp(-k \cdot LAI)] + \left(LW - 2\sigma T_{sv}^4 + \varepsilon\sigma T_{ss}^4\right)[1 - \exp(-k \cdot LAI)] \quad \text{(A1)}$$

$$Rn_s = [(1 - a_v)SW + LW]\exp(-k \cdot LAI) + \sigma T_{sv}^4 \cdot [1 - \exp(-k \cdot LAI)] - \varepsilon\sigma T_{ss}^4, \quad \text{(A2)}$$

where SW and LW are incoming short- and long-wave radiation respectively (see Figure 2), T_{ss} and T_{sv} are soil surface and leaf surface temperatures respectively, a_v is canopy average albedo, k is extinction coefficient, LAI is leaf area index, σ is Stefan-Boltzmann constant and ε is soil emissivity. The energy balance for the leaves can be written as:

$$\rho_w c_w l_f LAI \frac{dT_{sv}}{dt} = Rn_v - H_v - LE_v, \tag{A3}$$

where ρ_w and c_w are water density and specific heat (here we considered the leaf thermal properties similar to water), l_f is average leaf thickness, latent heat, LE_v, is the same as TR from equation (7) converted to energy units, and sensible heat, H_v, which is given by

$$H_v = \rho_a c_p \frac{(T_{sv} - T_{av})}{r_b}, \tag{A4}$$

where T_{av} is canopy air temperature, ρ_a is air density, c_p is specific heat of air at constant pressure and r_b is boundary layer resistance.

[42] Similarly, the energy balance for canopy air can be written as

$$h_c \rho_a c_p \frac{dT_{av}}{dt} = H_s + H_v - H_a, \tag{A5}$$

where, h_c is the canopy height. H_a and H_s are sensible heat from the soil to canopy air and from canopy air to atmosphere respectively, and are given by

$$H_a = \rho_a c_p \frac{T_{av} - T_a}{r_v + r_a} \tag{A6}$$

$$H_s = \rho_a c_p \frac{T_s|_{z=0} - T_{av}}{r_{ss}}, \tag{A7}$$

where T_a is the air temperature at a measurement height (see Figure 2), and r_v and r_a are the aerodynamic resistances from mean canopy height to canopy top and from canopy top to measurement height respectively, r_{ss} is aerodynamic resistance from soil to canopy air and T_s is soil temperature. In addition, the water vapor mass balance for canopy air is

$$h_c l_v \frac{d\rho_{av}}{dt} = LE_v + LE_s - LE_a, \tag{A8}$$

where ρ_{av} is water vapor concentration of canopy air, LE_s is evaporation from soil surface to canopy air expressed in energy units and l_v is latent heat of vaporization. LE_a is latent heat from canopy air to atmosphere given by

$$LE_a = \frac{l_v M_w}{R_g} \frac{1}{r_v + r_a} \left(\frac{e_{av}}{T_{av}} - \frac{e_a}{T_a} \right), \tag{A9}$$

where e_a is the vapor pressure at measurement height (saturation vapor pressure at due point, see Figure 2).

[43] Soil energy balance is calculated with a diffusion equation for heat flux in the soil:

$$\rho_s c_s \frac{\partial T_s}{\partial t} = \frac{\partial}{\partial z} K_T \frac{\partial T_s}{\partial z} - l_v E_s, \tag{A10}$$

where T_s is soil temperature, ρ_s and c_s are bulk soil (soil and water) density and specific heat respectively, K_T bulk soil (soil, water and air) thermal conductivity. Boundary conditions for equation (A10) are

$$K_T \frac{\partial T_s}{\partial z}\bigg|_{z=0} = G = Rn_s - H_s \tag{A11}$$

$$K_T \frac{\partial T_s}{\partial z}\bigg|_{z=Z} = 0, \tag{A12}$$

where G is ground heat flux and Z is domain size.

[44] Soil evaporation follows the algorithm described in *Campbell* [1985]. The water vapor flux within the soil, J_v, is given by

$$J_v = K_v \frac{\partial h_s}{\partial z}, \tag{A13}$$

where h_s is the fractional relative humidity in the soil and K_v is the conductivity for water vapor of the soil, which is given by [*Penman*, 1940]

$$K_v = 0.66 D_v (\theta_s - \theta) \rho_s, \tag{A14}$$

where D_v is vapor diffusivity in free air and ρ_s is vapor concentration in the soil pores. This linear diffusivity model tends to overestimate evaporation when compared to more sophisticated nonlinear models [*Suwa et al.*, 2004]. Under the simulated conditions, evaporation accounted for less then 10% of evapotranspiration, which makes the use of the linear model conservative and appropriate in this case. Evaporation can be written as

$$E_s = \frac{\partial J_v}{\partial z}. \tag{A15}$$

The aerodynamic resistances are calculated assuming an exponential profile for wind speed U and eddy diffusivity K_e [*Tuzet et al.*, 2003]:

$$U = U_{hc} \exp\left[\eta \left(\frac{z}{h_c} - 1 \right) \right] \tag{A16}$$

$$K_e = K_{e,hc} \exp\left[\eta \left(\frac{z}{h_c} - 1 \right) \right], \tag{A17}$$

where U_{hc} and $K_{e,hc}$ are wind speed and eddy diffusivity at the canopy top, and η is an extinction coefficient given by

$$\eta = h_c \left(\frac{c_d LAI}{2 l_c^2 h_c} \right)^{1/3}, \tag{A18}$$

where c_d is drag coefficient and l_c is the average leaf width. The aerodynamic resistance can be written as

$$r_{ss} = \int_{z_0}^{h_v} \frac{dz}{K_e} \tag{A19}$$

$$r_v = \int_{h_v}^{h_c} \frac{dz}{K_e} \tag{A20}$$

$$r_a = \int_{h_c}^{h_m} \frac{dz}{K_e}, \tag{A21}$$

where z_0 is the roughness length of soil surface, h_v mean canopy source/sink height and h_m is the measurement height. Finally, bulk soil boundary layer resistance can be written as

$$\frac{1}{r_b} = \frac{1}{h_c - z_0} \int_{z_0}^{h_c} \frac{U_{hc}^{0.5}}{C_t d_l^{0.5}} \exp\left[\frac{\eta}{2}\left(\frac{z}{h_c} - 1\right)\right] dz, \tag{A22}$$

where C_t is the transfer coefficient (C_t = 156.2).

[45] **Acknowledgments.** This study was supported by the U.S. Department of Energy (DOE) through the Office of Biological and Environmental Research (BER) Terrestrial Carbon Processes (TCP) program (grants 10509-0152, DE-FG02-00ER53015, and DE-FG02-95ER62083), by the National Science Foundation (NSF-EAR 0628342, NSF-EAR 0635787), and by BARD (IS-3861-06).

References

Bohrer, G., H. Mourad, T. A. Laursen, D. Drewry, R. Avissar, D. Poggi, R. Oren, and G. G. Katul (2005), Finite element tree crown hydrodynamics model (FETCH) using porous media flow within branching elements: A new representation of tree hydrodynamics, *Water Resour. Res.*, *41*, W11404, doi:10.1029/2005WR004181.

Brooks, J. R., F. C. Meinzer, R. Coulombe, and J. Gregg (2002), Hydraulic redistribution of soil water during summer drought in two contrasting Pacific Northwest coniferous forests, *Tree Physiol.*, *22*, 1107–1117.

Burgess, S. S. O., M. A. Adams, N. C. Turner, and C. K. Ong (1998), The redistribution of soil water by tree root systems, *Oecologia*, *115*, 306–311, doi:10.1007/s004420050521.

Caldwell, M. M., T. E. Dawson, and J. H. Richards (1998), Hydraulic lift: Consequences of water efflux from the roots of plants, *Oecologia*, *113*, 151–161, doi:10.1007/s004420050363.

Campbell, G. S. (1985), *Soil Physics With BASIC: Transport Models for Soil-Plant Systems*, Elsevier, Amsterdan.

Chuang, Y. L., R. Oren, A. L. Bertozzi, N. Phillips, and G. G. Katul (2006), The porous media model for the hydraulic system of a conifer tree: Linking sap flux data to transpiration rate, *Ecol. Modell.*, *191*, 447–468, doi:10.1016/j.ecolmodel.2005.03.027.

Davies, W. J., and J. H. Zhang (1991), Root signals and the regulation of growth and development of plants in drying soil, *Annu. Rev. Plant Physiol. Plant Mol. Biol.*, *42*, 55–76, doi:10.1146/annurev.pp.42.060191.000415.

Dawson, T. E. (1993), Hydraulic lift and water-use by plants—Implications for water-balance, performance and plant-plant interactions, *Oecologia*, *95*, 565–574, doi:10.1007/BF00317442.

Eamus, D., L. B. Hutley, and A. P. O'Grady (2001), Daily and seasonal patterns of carbon and water fluxes above a north Australian savanna, *Tree Physiol.*, *21*, 977–988.

Emerman, S. H., and T. E. Dawson (1996), Hydraulic lift and its influence on the water content of the rhizosphere: An example from sugar maple, acer saccharum, *Oecologia*, *108*, 273–278, doi:10.1007/BF00334651.

Feddes, R. A., et al. (2001), Modeling root water uptake in hydrological and climate models, *Bull. Am. Meteorol. Soc.*, *82*, 2797–2809.

Gedney, N., P. M. Cox, R. A. Betts, O. Boucher, C. Huntingford, and P. A. Stott (2006), Detection of a direct carbon dioxide effect in continental river runoff records, *Nature*, *439*, 835–838, doi:10.1038/nature04504.

Grant, R. F., R. L. Garcia, P. J. Pinter, D. Hunsaker, G. W. Wall, B. A. Kimball, and R. L. LaMorte (1995), Interaction between atmospheric CO_2 concentration and water deficit on gas exchange and crop growth: Testing of ecosys with data from the free air CO_2 enrichment (face) experiment, *Global Change Biol.*, *1*, 443–454, doi:10.1111/j.1365-2486.1995.tb00042.x.

Guswa, A. J., M. A. Celia, and I. Rodriguez-Iturbe (2004), Effect of vertical resolution on predictions of transpiration in water-limited ecosystems, *Adv. Water Resour.*, *27*, 467–480, doi:10.1016/j.advwatres.2004.03.001.

Hao, X. M., R. D. Zhang, and A. Kravchenko (2005), Effects of root density distribution models on root water uptake and water flow under irrigation, *Soil Sci.*, *170*, 167–174, doi:10.1097/01.ss.0000160031.00061.8b.

Hopmans, J. W. (2006), Soil physical properties, processes and associated root-soil interactions, in *Dryland Ecohydrology*, edited by P. D'Odorico and A. Porporato, pp. 13–29, Springer, Dordrecht, Netherlands.

Jackson, R. B., J. Canadell, J. R. Ehleringer, H. A. Mooney, O. E. Sala, and E. D. Schulze (1996), A global analysis of root distributions for terrestrial biomes, *Oecologia*, *108*, 389–411, doi:10.1007/BF00333714.

Jones, H. G., and R. A. Sutherland (1991), Stomatal control of xylem embolism, *Plant Cell Environ.*, *14*, 607–612, doi:10.1111/j.1365-3040.1991.tb01532.x.

Koster, R. D., et al. (2004), Regions of strong coupling between soil moisture and precipitation, *Science*, *305*, 1138–1140, doi:10.1126/science.1100217.

Lafolie, F., L. Bruckler, and F. Tardieu (1991), Modeling root water potential and soil root water transport. 1. Model presentation, *Soil Sci. Soc. Am. J.*, *55*, 1203–1212.

Laio, F., P. D'Odorico, and L. Ridolfi (2006), An analytical model to relate the vertical root distribution to climate and soil properties, *Geophys. Res. Lett.*, *33*, L18401, doi:10.1029/2006GL027331.

Lee, J. E., R. S. Oliveira, T. E. Dawson, and I. Fung (2005), Root functioning modifies seasonal climate, *Proc. Natl. Acad. Sci. U. S.A.*, *102*, 17,576–17,581, doi:10.1073/pnas.0508785102.

Li, K. Y., De R. Jong, and J. B. Boisvert (1999), Comparison of root uptake models, paper presented at 10th International Soil Conservation Organization Meeting, Natl. Soil Erosion Res. Lab., Agric. Res. Serv., U.S. Dep. of Agric., West Lafayette, Indiana.

Mendel, M., S. Hergarten, and H. J. Neugebauer (2002), On a better understanding of hydraulic lift: A numerical study, *Water Resour. Res.*, *38*(10), 1183, doi:10.1029/2001WR000911.

Milly, P. C. D., K. A. Dunne, and A. V. Vecchia (2005), Global pattern of trends in streamflow and water availability in a changing climate, *Nature*, *438*, 347–350, doi:10.1038/nature04312.

Niklas, K. J. (1992), *Plant Biomechanics: An Engineering Approach to Plant Form and Function*, Univ. of Chicago Press, Chicago, Ill.

Oliveira, R. S., T. E. Dawson, and S. S. O. Burgess (2005a), Evidence for direct water absorption by the shoot of the desiccation-tolerant plant vellozia flavicans in the savannas of central Brazil, *J. Trop. Ecol.*, *21*, 585–588, doi:10.1017/S0266467405002658.

Oliveira, R. S., T. E. Dawson, S. S.O. Burgess, and D. C. Nepstad (2005b), Hydraulic redistribution in three amazonian trees, *Oecologia*, *145*, 354–363, doi:10.1007/s00442-005-0108-2.

Penman, H. L. (1940), Gas and vapour movements in the soil I. The diffusion of vapours through porous solids, *J. Agric. Sci.*, *30*, 437–462.

Prior, L. D., D. Eamus, and G. A. Duff (1997), Seasonal and diurnal patterns of carbon assimilation, stomatal conductance and leaf water potential in eucalyptus tetrodonta saplings in a wet-dry savanna in northern Australia, *Aust. J. Bot.*, *45*, 241–258, doi:10.1071/BT96017.

Puma, M. J., M. A. Celia, I. Rodriguez-Iturbe, and A. J. Guswa (2005), Functional relationship to describe temporal statistics of soil moisture averaged over different depths, *Adv. Water Resour.*, *28*, 553–566, doi:10.1016/j.advwatres.2004.08.015.

Redinger, G. J., G. S. Campbell, K. E. Saxton, and R. I. Papendick (1984), Infiltration-rate of slot mulches—Measurement and numerical-simulation, *Soil Sci. Soc. Am. J.*, *48*, 982–986.

Richards, L. (1931), Capillary conduction of liquid through porous medium, *Physics*, *1*, 318–333.

Siqueira, M. B., G. G. Katul, D. A. Sampson, P. C. Stoy, J. Y. Juang, H. R. McCarthy, and R. Oren (2006), Multiscale model intercomparisons of CO_2 and H_2O exchange rates in a maturing southeastern us pine forest, *Global Change Biol.*, *12*, 1189–1207, doi:10.1111/j.1365-2486.2006.01158.x.

Skaggs, T. H., M. T. van Genuchten, P. J. Shouse, and J. A. Poss (2006), Macroscopic approaches to root water uptake as a function of water and salinity stress, *Agric. Water Manage.*, *86*, 140–149, doi:10.1016/j.agwat.2006.06.005.

Sperry, J. S. (2000), Hydraulic constraints on plant gas exchange, *Agric. For. Meteorol.*, *104*, 13–23, doi:10.1016/S0168-1923 (00)00144-1.

Sperry, J. S., F. R. Adler, G. S. Campbell, and J. P. Comstock (1998), Limitation of plant water use by rhizosphere and xylem conductance: Results from a model, *Plant Cell Environ.*, *21*, 347–359, doi:10.1046/j.1365-3040.1998.00287.x.

Steudle, E. (2000), Water uptake by plant roots: An integration of views, *Plant Soil*, *226*, 45–56, doi:10.1023/A:1026439226716.

Suwa, M., G. G. Katul, R. Oren, J. Andrews, J. Pippen, A. Mace, and W. H. Schlesinger (2004), Impact of elevated atmospheric CO_2 on forest floor respiration in a temperate pine forest, *Global Biogeochem. Cycles*, *18*, GB2013, doi:10.1029/2003GB002182.

Tardieu, F., and W. J. Davies (1993), Integration of hydraulic and chemical signaling in the control of stomatal conductance and water status of droughted plants, *Plant Cell Environ.*, *16*, 341–349, doi:10.1111/j.1365-3040.1993.tb00880.x.

Tardieu, F., J. Zhang, and W. J. Davies (1992), What information is conveyed by an ABA signal from maize roots in drying field soil, *Plant Cell Environ.*, *15*, 185–191, doi:10.1111/j.1365-3040.1992.tb01472.x.

Tuzet, A., A. Perrier, and R. Leuning (2003), A coupled model of stomatal conductance, photosynthesis and transpiration, *Plant Cell Environment*, *26*, 1097–1116, doi:10.1111/j.1365-3040.1992.tb01472.x.

Tyree, M. T., and J. S. Sperry (1988), Do woody-plants operate near the point of catastrophic xylem dysfunction caused by dynamic water-stress—Answers from a model, *Plant Physiol.*, *88*, 574–580.

Vrugt, J. A., M. T. van Wijk, J. W. Hopmans, and J. Simunek (2001), One-, two-, and three-dimensional root water uptake functions for transient modeling, *Water Resour. Res.*, *37*, 2457–2470.

Williams, K., M. M. Caldwell, and J. H. Richards (1993), The influence of shade and clouds on soil-water potential—The buffered behavior of hydraulic lift, *Plant Soil*, *157*, 83–95, doi:10.1007/BF02390230.

Yoder, C. K., and R. S. Nowak (1999), Soil moisture extraction by evergreen and drought-deciduous shrubs in the Mojave desert during wet and dry years, *J. Arid Environ.*, *42*, 81–96, doi:10.1006/jare.1999.0504.

G. Katul and M. Siqueira, Nicholas School of the Environment and Earth Sciences, Duke University, Box 90328, Durham, NC 27708-0328, USA. (bs4@duke.edu)

A. Porporato, Department of Civil and Environmental Engineering, Pratt School of Engineering, Duke University, Durham, NC 27708, USA.